

# Binding Pocket Alterations in Dihydrofolate Synthase Confer Resistance to *para*-Aminosalicylic Acid in Clinical Isolates of *Mycobacterium tuberculosis*

Fei Zhao,<sup>a,b</sup> Xu-De Wang,<sup>a</sup> Luke N. Erber,<sup>c</sup> Ming Luo,<sup>d</sup> Ai-zhen Guo,<sup>b</sup> Shan-shan Yang,<sup>a</sup> Jing Gu,<sup>a</sup> Breanna J. Turman,<sup>c</sup> Yun-rong Gao,<sup>e</sup> Dong-fang Li,<sup>f,g</sup> Zong-qiang Cui,<sup>a</sup> Zhi-ping Zhang,<sup>a</sup> Li-jun Bi,<sup>e</sup> Anthony D. Baughn,<sup>c</sup> Xian-En Zhang,<sup>e</sup> Jiao-Yu Deng<sup>a</sup>

Key Laboratory of Agricultural and Environmental Microbiology, Wuhan Institute of Virology, Chinese Academy of Sciences, Wuhan, China<sup>a</sup>; State Key Laboratory of Agricultural Microbiology, College of Life Science and Technology, Huazhong Agriculture University, Wuhan, China<sup>b</sup>; Department of Microbiology, University of Minnesota, Minneapolis, Minnesota, USA<sup>c</sup>; Chongqing Institute of Tuberculosis Prevention and Treatment, Chongqing, China<sup>d</sup>; National Laboratory of Biomacromolecules, Institute of Biophysics, Chinese Academy of Sciences, Beijing, China<sup>e</sup>; Shenzhen Key Laboratory of Unknown Pathogen Identification, Shenzhen, China<sup>f</sup>; BGI-Tianjin, Tianjin, China<sup>g</sup>

**The mechanistic basis for the resistance of *Mycobacterium tuberculosis* to *para*-aminosalicylic acid (PAS), an important agent in the treatment of multidrug-resistant tuberculosis, has yet to be fully defined. As a substrate analog of the folate precursor *para*-aminobenzoic acid, PAS is ultimately bioactivated to hydroxy dihydrofolate, which inhibits dihydrofolate reductase and disrupts the operation of folate-dependent metabolic pathways. As a result, the mutation of dihydrofolate synthase, an enzyme needed for the bioactivation of PAS, causes PAS resistance in *M. tuberculosis* strain H37Rv. Here, we demonstrate that various missense mutations within the coding sequence of the dihydropteroyl (H<sub>2</sub>Pte) binding pocket of dihydrofolate synthase (FolC) confer PAS resistance in laboratory isolates of *M. tuberculosis* and *Mycobacterium bovis*. From a panel of 85 multidrug-resistant *M. tuberculosis* clinical isolates, 5 were found to harbor mutations in the *folC* gene within the H<sub>2</sub>Pte binding pocket, resulting in PAS resistance. While these alterations in the H<sub>2</sub>Pte binding pocket resulted in reduced dihydrofolate synthase activity, they also abolished the bioactivation of hydroxy dihydropteroyl to hydroxy dihydrofolate. Consistent with this model for abolished bioactivation, the introduction of a wild-type copy of *folC* fully restored PAS susceptibility in *folC* mutant strains. Confirmation of this novel PAS resistance mechanism will be beneficial for the development of molecular method-based diagnostics for *M. tuberculosis* clinical isolates and for further defining the mode of action of this important tuberculosis drug.**

Two billion people worldwide are latently infected with *Mycobacterium tuberculosis* (1). Each year, this immense reservoir of infected individuals yields 9 million new cases of active tuberculosis (TB), resulting in the transmission of tubercle bacilli to tens of millions of naive individuals and 2 million TB-related deaths (1). The emergent spread of multidrug-resistant (MDR) (resistant to isoniazid and rifampin) and extensively drug-resistant (XDR) (resistant to isoniazid, rifampin, quinolones, and any second-line injectable drug) strains of *M. tuberculosis* now threatens the efficacy of existing antitubercular therapies (2, 3). In high-TB-burden countries, the reported case rates of MDR-TB doubled between 2009 and 2011, and to date, XDR-TB has been reported in 84 different countries (3). Defining the underlying molecular and biochemical mechanisms of TB drug resistance is critical to facilitate the development of novel diagnostic tools and to guide target-based discovery of novel therapeutic agents.

*para*-Aminosalicylic acid (PAS) was first reported by Lehmann in 1946 (4) and followed streptomycin as the second therapeutic agent used in the treatment of TB. Despite nearly 70 years of clinical use of PAS, the mechanistic basis for the susceptibility and resistance of *M. tuberculosis* to this drug has not been fully defined. Based on the structural similarity of PAS to the folate precursor *para*-aminobenzoic acid (PABA) and the observation that the antitubercular action of PAS can be fully antagonized by exogenous PABA (5), PAS was initially thought to interfere with folate synthesis through the inhibition of dihydropteroyl synthase activity (DHPS/FolP1), similar to the action of many sulfonamides. However, subsequent enzymology with purified recombinant FolP1

demonstrated that PAS is a poor inhibitor of DHPS activity (6). Recently, PAS has been shown to function as an alternate substrate for FolP1 with the formation of an analog of dihydropteroyl (H<sub>2</sub>Pte), hydroxy dihydropteroyl (H<sub>2</sub>PtePAS), which can be glutaminated by dihydrofolate synthase (DHFS/FolC) to form the dihydrofolate (H<sub>2</sub>Pte-Glu) analog hydroxy dihydrofolate (H<sub>2</sub>PtePAS-Glu) (7). H<sub>2</sub>PtePAS-Glu can then inhibit the activity of dihydrofolate reductase (DfrA), resulting in the growth arrest of *M. tuberculosis* due to a limitation in its ability to synthesize tetrahydrofolate (8). Consistent with this model for the PAS mode of action, overexpression of an alternate enzyme with dihydrofolate reductase activity, RibD, confers resistance to this drug (8). Interestingly, loss-of-function mutations in *thyA*, which encodes a folate-dependent thymidylate synthase, have been associated with PAS resistance by an undefined mechanism in both laboratory and clinical isolates of *M. tuberculosis* (9, 10). As only one-third of

Received 16 August 2013 Returned for modification 7 October 2013

Accepted 12 December 2013

Published ahead of print 23 December 2013

Address correspondence to Jiao-Yu Deng, dengjy@wh.iov.cn., or Xian-En Zhang, xzhang@wh.iov.cn.

Supplemental material for this article may be found at <http://dx.doi.org/10.1128/AAC.01775-13>.

Copyright © 2014, American Society for Microbiology. All Rights Reserved.  
doi:10.1128/AAC.01775-13

PAS-resistant clinical isolates have been found to harbor *thyA* mutations, and not all *thyA* mutations are associated with PAS resistance (10–12), additional PAS resistance alleles have yet to be identified. Very recently, Zheng et al. (8) described a spontaneous PAS-resistant isolate of *M. tuberculosis* H37Rv harboring a substitution mutation in *folC* that was responsible for PAS resistance, suggesting that PAS resistance can also be mediated by alterations in dihydrofolate synthase.

To better understand the mechanistic basis for PAS susceptibility and resistance in *M. tuberculosis*, we characterized several PAS-resistant laboratory and clinical isolates using genome-wide and targeted sequencing-based methods. Using this approach, we identified a number of single nucleotide missense polymorphisms clustered within the coding sequence for the H<sub>2</sub>Pte binding pocket of FolC that were associated with PAS resistance. This association was confirmed by complementation and gene replacement studies in both laboratory and clinical isolates. Finally, biochemical studies were performed on purified recombinant wild-type and variant forms of FolC to assess the consequences of changes in the H<sub>2</sub>Pte binding pocket for DHFS activity using H<sub>2</sub>Pte and H<sub>2</sub>PtePAS as substrates. Based on these studies, a novel mechanism of PAS resistance in clinical isolates of *M. tuberculosis* was confirmed whereby variant forms of FolC show diminished activation of H<sub>2</sub>PtePAS to H<sub>2</sub>PtePAS-Glu. This work will be beneficial in the further development of molecular diagnostic tools for assessing PAS resistance, and it also provides new insights into studies of mechanisms of PAS action.

## MATERIALS AND METHODS

**Bacterial strains, plasmids, and growth conditions.** Clinical *M. tuberculosis* strains, *M. tuberculosis* strain H37Ra, *Mycobacterium bovis* BCG, and their derivatives were cultured in Middlebrook 7H9 broth (Difco) supplemented with 10% (vol/vol) oleic acid-albumin-dextrose-catalase (OADC) (Difco), 0.5% (vol/vol) glycerol, and 0.05% (vol/vol) Tween 80 (Sigma) or on 7H10 agar medium (Difco) supplemented with 10% (vol/vol) OADC and 0.5% (vol/vol) glycerol. *Mycobacterium smegmatis* strain mc<sup>2</sup>155 was grown with Middlebrook 7H9 broth or 7H10 agar medium (Difco) supplemented with 0.5% (vol/vol) glycerol, and 0.05% (vol/vol) Tween 80 was added to each culture. *Escherichia coli* strains HB101 and BL21(DE3) were grown with Luria-Bertani medium (Difco). Plasmids pMAL-c2X (New England BioLabs), pET-28a (Novagen), pMV361, and pMV261 were used for the construction of expression plasmids. Antibiotics were added to the growth media as necessary: hygromycin at 75 µg/ml for mycobacteria and 150 µg/ml for *E. coli*, ampicillin at 100 µg/ml for *E. coli*, and kanamycin at 25 µg/ml for mycobacteria and 50 µg/ml for *E. coli*.

**Identification of PAS resistance alleles.** *M. tuberculosis* H37Ra and *M. bovis* BCG were grown in supplemented 7H9 medium to an optical density at 600 nm (OD<sub>600</sub>) of ~0.8, collected by centrifugation (4,000 × g, 15 min, at room temperature), and resuspended in fresh medium at a concentration of 10<sup>8</sup> CFU/ml. Subsequently, 200 µl of concentrated bacterial cells was spread onto supplemented 7H10 agar plates containing 1, 4, and 16 µg/ml PAS and incubated at 37°C for 3 weeks for the selection of PAS-resistant mutants. Single colonies were purified, and liquid cultures were grown for the extraction of genomic DNA and determination of PAS MICs (with MIC defined as the lowest concentration of compound required to inhibit 99% of bacterial growth over 3 weeks of incubation at 37°C) according to the established protocols (13–15). PCR-free DNA libraries for full-genome sequencing were constructed from the genomic DNA of selected strains using a TruSeq DNA kit (Illumina, Inc.) according to the manufacturer's protocol, with an average insert size of 350 bp for each sample, and these were assayed using the Illumina MiSeq or HiSeq 2000 sequencing systems. A base-calling pipeline (version HC1.4/

RTA1.12) was used to process the raw fluorescent images and call sequences. An average of 520 Mb of data for each sample was generated, representing >100-fold sequence coverage per genome. High-quality paired-end reads were mapped to the reference H37Ra genome (GenBank NC\_009525) using SOAP2 (16) or Geneious 6.0 (Biomatters Ltd., Auckland, New Zealand). Single nucleotide polymorphisms were independently verified by the sequencing of PCR amplicons of the respective loci. Genomic DNAs of PAS-resistant strains that were not assessed by full-genome sequencing, including genomic DNA from clinical *M. tuberculosis* isolates (10 drug-susceptible and 85 MDR isolates obtained from the Chongqing Institute of Tuberculosis Prevention and Treatment), were assessed by targeted sequencing of PCR amplicons of loci associated with PAS resistance. The primers used in the targeted sequencing are described in Table S1 in the supplemental material.

**Genetic manipulation of mycobacterial strains.** *FolC* was amplified from wild-type *M. tuberculosis* H37Ra genomic DNA using PCR with the primer pair FolCBamHIFP and FolCHindIIIIRP (see Table S1 in the supplemental material). The purified amplicon was digested with BamHI and HindIII and ligated to BamHI-HindIII-cut pMV261, yielding pMV261-FolC. PAS-resistant *M. tuberculosis* and *M. bovis* BCG strains were transformed with sequence-confirmed pMV261-FolC according to the established protocols (14) and plated on 7H10 medium containing kanamycin. After 3 weeks of incubation at 37°C, single colonies were purified and liquid cultures were prepared for the extraction of genomic DNA and determination of PAS MICs. The presence of pMV261-FolC was verified by PCR amplification using primers specific for pMV261 (JDFF and JDRP) (see Table S1 in the supplemental material).

A modified strategy for phage-mediated allelic exchange (17) was used to construct *M. tuberculosis* H37Ra derivatives containing the clinically derived *folC* alleles I43A and I43T. Briefly, *folC* alleles were cloned into pMV361 and used to transform *M. tuberculosis* H37Ra. The native copy of *folC* was deleted by specialized transduction using phAE159 containing a Δ*folC* allelic exchange substrate (see Fig. S1 in the supplemental material). The deletion of the native copy of *folC* was verified by PCR as described in Fig. S1.

**Purification of recombinant FolP1 and FolC.** FolP1 was amplified from *M. tuberculosis* H37Ra genomic DNA using the primers FolPNcoIFP and FolPHindIIIIRP (see Table S1 in the supplemental material) and was cloned into pET28a, yielding pET28a-FolP1 to introduce an N-terminal hexahistidine tag. Following sequence verification, pET28a-FolP1 was used to transform *E. coli* BL21(DE3). The cells were grown at 37°C in Luria-Bertani broth to an OD<sub>600</sub> of ~0.6, isopropyl-β-D-thiogalactopyranoside (IPTG) was added to 0.2 mM, and the cells were incubated at 16°C overnight. Following induction, the bacterial cells were harvested by centrifugation, resuspended in 50 mM Tris-HCl, 0.5 M NaCl, 20 mM imidazole (pH 8.0), disrupted by sonication, and clarified by centrifugation. Supernatant fluid was mixed with prewashed nickel-nitrilotriacetic acid HisTrap HP affinity resin (GE Healthcare) at 4°C overnight. Nonspecifically bound protein was removed by washing the resin with 50 mM Tris-HCl, 0.5 M NaCl, and 60 mM imidazole (pH 8.0). Recombinant FolP1 was eluted with 50 mM Tris-HCl, 0.5 M NaCl, and 400 mM imidazole (pH 8.0), and analyzed by SDS-PAGE.

Wild-type and mutant (I43T, R49W, E153A, and A183P mutations) *folC* genes were amplified from genomic DNA of the respective *M. tuberculosis* strains using the primers FolCBamHIFP and FolCHindIIIIRP (see Table S1 in the supplemental material). The amplicons were digested with BamHI and HindIII and cloned into pMAL-c2X (New England BioLabs) to introduce a maltose binding protein (MBP) tag linked by a factor Xa cleavage site. After sequence verification, plasmids were used to transform *E. coli* BL21(DE3). The cells were grown at 37°C in Luria-Bertani broth to an OD<sub>600</sub> of ~1.0, IPTG was added to 0.1 mM, and the cells were incubated at 16°C overnight. The bacterial cells were harvested by centrifugation, resuspended in column buffer (CB) (50 mM Tris-HCl, 0.5 M NaCl [pH 8.0]), and disrupted by sonication. Recombinant FolC proteins were first purified over an amylose resin column (product no. E8021, New

England BioLabs). In brief, the column was prewashed with 10 volumes of CB, crude extract was loaded, the column was washed with 10 volumes of CB, and recombinant MBP-tagged FolC was eluted with CB containing 10 mM maltose. To remove the MBP tag, the samples were incubated with factor Xa at 23°C for 6 h in 20 mM HEPES (pH 8.0), 100 mM NaCl, and 2 mM CaCl<sub>2</sub>. Finally, the cleavage mixtures were dialyzed against 50 mM phosphate buffer (PB) (pH 8.0). The samples were loaded on a HiTrap DEAE FF column (GE Healthcare), and a step gradient from 50 mM to 1 M NaCl in PB was applied to elute FolC. The fractions were analyzed by SDS-PAGE. Recombinant FolC was found to elute with 300 mM NaCl.

**Enzymatic assays.** Dihydrofolate synthase activities of wild-type FolC and its variants using H<sub>2</sub>Pte (Schircks Laboratories) as a substrate were measured as previously described (7). The standard reactions consisted of 1 μM FolC protein, 110 mM Tris-55 mM glycine (pH 9.5), 11 mM MgCl<sub>2</sub>, 5 mM dithiothreitol (DTT), 200 mM KCl, 50 mM NaCl, 10% glycerol, 1 mM L-glutamate, 5 mM ATP, and 100 μM H<sub>2</sub>Pte. The reactions were carried out at 37°C for 1 h in triplicate and were stopped by the addition of EDTA to a final concentration of 50 mM. The reaction mixtures were injected onto a Phenomenex Luna 3-μm C<sub>18</sub> 100-Å liquid chromatography (LC) column (50 by 2 mm) (2) in an UltiMate 3000 ultrahigh-performance liquid chromatography (UHPLC) system (Thermo Fisher Scientific). The samples were eluted with a gradient from 95% buffer A (H<sub>2</sub>O plus 0.1% acetic acid) and 5% buffer B (acetonitrile plus 0.1% acetic acid) to 5% buffer A and 95% buffer B for 15 min, at a flow rate of 0.3 ml/min. The peak of H<sub>2</sub>Pte-Glu was measured by UV absorbance (A<sub>284</sub>). The peak areas of H<sub>2</sub>Pte-Glu were converted to concentrations by comparison against an H<sub>2</sub>Pte-Glu analytical standard (Schircks Laboratories).

The dihydrofolate synthase activities of wild-type FolC and its mutants using H<sub>2</sub>PtePAS as a substrate were also measured according to the above method. H<sub>2</sub>PtePAS was enzymatically synthesized as previously described (7). Briefly, a reaction mixture containing 1.2 μM FolP1, 40 mM Tris-20 mM glycine (pH 9.5), 5 mM MgCl<sub>2</sub>, 1 mM DTT, 200 mM NaCl, appropriate amounts of 6-hydroxymethyl-7,8-pterin pyrophosphate (H<sub>2</sub>PtePP), and 250 μM PAS was incubated at 37°C for 1 h. Next, FolP1 was removed by passing through a 10-kDa Microcon centrifugal filter, and the mixture was subsequently used as a substrate for FolC. H<sub>2</sub>PtePAS and H<sub>2</sub>PtePAS-Glu were identified by UHPLC as described above and confirmed by electrospray ionization/mass spectrometry (ESI/MS) with an in-line LCQ Fleet ion trap mass spectrometer (Thermo Fisher Scientific). The ESI/MS working parameters were as follows: 4 kV capillary voltage, 300°C heat block temperature for analysis, and the nitrogen drying and nebulizer gases were set at 5 liter/min. All MS data were acquired in a scan range between 100 and 1,000 *m/z* under the negative ionization mode.

To compare the catalytic rate of wild-type FolC for H<sub>2</sub>PtePAS and H<sub>2</sub>Pte, these two compounds were enzymatically synthesized as described above. The reaction mixture contained 1.2 μM FolP1, 40 mM Tris-20 mM glycine (pH 9.5), 5 mM MgCl<sub>2</sub>, 1 mM DTT, 200 mM NaCl, appropriate amounts of H<sub>2</sub>PtePP, and 250 μM PAS or PABA. The reaction mixture was incubated at 37°C until no increment of product accumulation was detected by high-performance liquid chromatography (HPLC). FolP1 was removed by passing through a 10-kDa Microcon centrifugal filter, and 325 μl of the remaining reaction mixture was used as a substrate for FolC. The concentration of H<sub>2</sub>Pte in the FolP1 reaction mixture was estimated by a comparison of the peak area of H<sub>2</sub>Pte in the mixture with that of the standard compound, and the concentration of H<sub>2</sub>PtePAS was assumed to be the same as that of H<sub>2</sub>Pte since the same amount of H<sub>2</sub>PtePP was consumed. The FolC reaction mixture contained 0.5 μM FolC protein, 2.5 mM ATP, and 0.5 mM L-glutamate in 100 mM Tris-50 mM glycine (pH 9.5), 10 mM MgCl<sub>2</sub>, 5 mM DTT, 100 mM KCl, 50 mM NaCl, 10% glycerol, and about 20 μM H<sub>2</sub>Pte or H<sub>2</sub>PtePAS. After incubation at 37°C for the proper times, the mixture was injected onto a Phenomenex Luna 3-μm C<sub>18</sub> 100-Å LC column (75 by 3 mm) (2) in an UltiMate 3000 UHPLC system linked with the LCQ Fleet. The samples were eluted with a gradient from 95% buffer A (H<sub>2</sub>O plus 0.1% acetic acid) and 5% buffer

B (acetonitrile plus 0.1% acetic acid) to 73% buffer A and 27% buffer B for 10 min, at a flow rate of 0.3 ml/min. Substrate consumption and product formation were determined by HPLC-MS as described above.

**Antagonism of PAS activity by H<sub>2</sub>Pte.** *M. tuberculosis* H37Ra was grown in 7H9 medium to mid-log phase (OD<sub>600</sub>, ~0.5), collected, and resuspended in fresh 7H9 medium to a density of OD<sub>600</sub> of ~0.1. Next, 200 μl of bacterial cells was aliquoted into 96-well plates. PAS (0.1 μg/ml) was added (except in the no-drug controls) in combination with different concentrations of H<sub>2</sub>Pte (0, 0.1, 0.3, 1, 3, and 10 μg/ml). The plates were incubated at 37°C without shaking. An XTT [2,3-bis(2-methoxy-4-nitro-5-sulphophenyl)-2H-tetrazolium-5-carboxanilide inner salt] reduction assay was performed to determine the survival of bacterial cells at 36 h, as previously described (18). The MICs of PAS for the wild-type *M. tuberculosis* H37Ra in the presence of different concentrations of H<sub>2</sub>Pte (3 and 10 μg/ml) were also determined.

## RESULTS

**Characterization of mutations associated with PAS resistance in *M. tuberculosis*.** In order to characterize novel alleles associated with PAS resistance, *M. tuberculosis* H37Ra and *M. bovis* BCG were plated on medium containing PAS at concentrations of 1, 4, and 16 μg/ml. For *M. tuberculosis* H37Ra, colonies arose at a frequency of  $5 \times 10^{-7}$  on 1 μg/ml PAS,  $2 \times 10^{-7}$  on 4 μg/ml PAS, and  $2 \times 10^{-8}$  on 16 μg/ml PAS. For *M. bovis* BCG, colonies arose at a frequency of  $3 \times 10^{-7}$  on 1 μg/ml PAS,  $2 \times 10^{-7}$  on 4 μg/ml PAS, and  $<2 \times 10^{-8}$  on 16 μg/ml PAS. Forty-three *M. tuberculosis* H37Ra PAS-resistant (PAS<sup>r</sup>) isolates and 23 *M. bovis* BCG PAS<sup>r</sup> isolates were chosen for further characterization (Table 1). Genome sequencing was performed on 16 of the spontaneous PAS<sup>r</sup> isolates of *M. tuberculosis* H37Ra and the parental strain. Comparative genomic analysis revealed that 11 strains harbored an A-to-C transversion within codon 153 of *folC* (GAG to GCG, resulting in E153A). In addition, two other strains harbored an A-to-G transition at codon 73 of *folC* (AAC to AGC, resulting in N73S). Targeted sequencing of *folC*, *folP1*, and *dfrA*, *ribD*, and *thyA* (previously linked to PAS resistance) (9–12) was performed on the remaining 50 spontaneous PAS<sup>r</sup> mutants. As shown in Table 1, an additional 32 strains had mutations within the *folC* gene, and 6 strains were found to have mutations within the *thyA* gene. No strains were found to harbor mutations in *dfrA* or *ribD*. Mutations were not identified in 15 of the strains that were analyzed by targeted sequencing, indicating the existence of additional PAS resistance alleles (Table 1).

From whole-genome and targeted sequencing, 67% (29/43) of the *M. tuberculosis* H37Ra spontaneous PAS<sup>r</sup> isolates and 70% (16/23) of the *M. bovis* BCG spontaneous PAS<sup>r</sup> isolates had mutations in *folC*, representing nine unique missense mutations (R49W, N73S, S150R, S150G, F152S, F152L, E153A, E153G, and A183P) that map to six positions that are invariant among mycobacterial FolC orthologs (see Fig. S2A in the supplemental material). Alignment of the protein sequences revealed that these six residues are also very highly conserved in FolC throughout prokaryotic species (see Fig. S2A and B). The crystal structures of *M. tuberculosis* FolC and those from other phylogenetically distinct species (*Lactobacillus casei*, *Yersinia pestis*, *Thermotoga maritima*, and *E. coli*) have been determined and show a remarkable degree of structural conservation (19–23). As shown in Fig. 1A and B, all of the identified *folC* mutations, except N73, were located within the α1-α2/α4-α5 helix bundle of the FolC N terminus. This four-helix bundle was mainly linked through hydrophobic interactions, and two residues (A183 and F152) are involved in the link-

TABLE 1 Mutations associated with PAS resistance in laboratory and clinical isolates of the *M. tuberculosis* complex

Strain(s)	PAS resistance <sup>b</sup>	No. of isolates	<i>folC</i> codon (mutation) <sup>c</sup>	<i>thyA</i> codon (mutation)
<i>M. tuberculosis</i> H37Ra				
ZF-1, <sup>a</sup> ZF-6, ZF-12, ZF-18, <sup>a</sup> ZF-26, <sup>a</sup> LNE-34, LNE-38, LNE-99	R	8	WT	WT
ZF-7, <sup>a</sup> ZF-8, <sup>a</sup> ZF-10, <sup>a</sup> ZF-11, <sup>a</sup> ZF-14, <sup>a</sup> ZF-15, <sup>a</sup> ZF-16, ZF-19, ZF-20, <sup>a</sup> ZF-21, <sup>a</sup> ZF-22, <sup>a</sup> ZF-23, ZF-24, <sup>a</sup> ZF-25, <sup>a</sup> LNE-1, LNE-7, LNE-10, LNE-12	R	18	GAG→GCG (E153A)	WT
ZF-13, ZF-17, LNE-6	R	3	GAG→GGG (E153G)	WT
ZF-4, ZF-9	R	2	TTC→TCC (F152S)	WT
ZF-5	R	1	TTC→CTC (F152L)	WT
ZF-2	R	1	AGC→AGG (S150R)	WT
ZF-3	R	1	AGC→GGC (S150G)	WT
LNE-3, <sup>a</sup> LNE-32, <sup>a</sup> LNE-39	R	3	AAC→AGC (N73S)	WT
LNE-47, BJT-77	R	2	WT	AAC→AAA (N134K)
LNE-48, LNE-93	R	2	WT	CAT→AAT (H147N)
LNE-51	R	1	WT	ACC→ATC (T22I)
LNE-54	R	1	WT	GGG→AGG (G15R)
<i>M. bovis</i> BCG				
ZF-33, ZF-42, ZF-44, ZF-46, ZF-47, ZF-48, ZF-49	R	7	WT	WT
ZF-27, ZF-29, ZF-30, ZF-31, ZF-35, ZF-36, ZF-37, ZF-38, ZF-39, ZF-40, ZF-41, ZF-43, ZF-45	R	13	GCC→CCC (A183P)	WT
ZF-28, ZF-32, ZF-34	R	3	CGG→TGG (R49W)	WT
Non-MDR <i>M. tuberculosis</i> clinical isolates				
MDR <i>M. tuberculosis</i> clinical isolates	ND	10	WT	WT
Q274, 501063	R	2	GAG→GGG (E40G)	WT
Q449, 1314	R	2	ATC→GCT (I43T)	WT
Q36	R	1	ATC→ACC (I43A)	WT
Q296	TBD	1	GGC→AGC (G111S)	WT
504036	TBD	1	GAC→GCC (D112A)	WT
Q93	TBD	1	CGG→TGG (R410W)	WT

<sup>a</sup> Strains analyzed by whole-genome sequencing.

<sup>b</sup> R, resistant (MIC > 0.125 μg/ml PAS); ND, not determined; TBD, to be determined.

<sup>c</sup> WT, identical to wild-type gene.

age of hydrophobic networks between  $\alpha 1$  and  $\alpha 5$ . The  $\alpha 1$ - $\alpha 2$  loop and the  $\alpha 4$ - $\alpha 5$  loop form an intersection, which is locked by two pairs of salt bridges, one pair between R49 and E153 and the other pair between R37 and D135. The first pair of salt bridges is responsible for the linkage between  $\alpha 1$  and  $\alpha 5$ , and the second pair is responsible for the linkage between  $\alpha 2$  and  $\alpha 4$ .

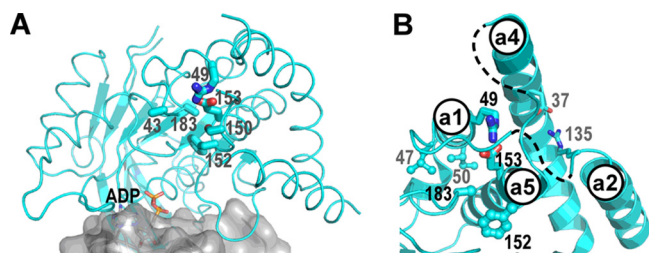


FIG 1 (A) Ribbon diagram of the N-domain FolC (PDB code 2VOS). The locations of six mutations are shown as thick colored bands (Ile43, Arg49, Ser150, Phe152, Glu153, and Ala183), while the ADP is shown as fine bands. (B) As shown, all the mutated residues either reside in the H<sub>2</sub>Pte binding loop ( $\alpha 1$ - $\alpha 2$ , residues 36 to 50) or are situated in the  $\alpha 4$ - $\alpha 5$  loop. The residue Glu40 was not included in the model.

**FolC H<sub>2</sub>Pte binding pocket mutations are associated with PAS resistance in *M. tuberculosis* clinical isolates.** To determine the clinical significance of *folC* mutations for PAS resistance, 95 recent clinical isolates of *M. tuberculosis* (10 drug-susceptible strains and 85 MDR strains) were assessed for *folC* mutations by targeted DNA sequencing (Table 1). As expected, all *folC* alleles from the drug-susceptible strains showed full sequence conservation with H37Rv *folC*. Among the 85 MDR strains, 8 had missense mutations within *folC* corresponding to E40G (two isolates), I43A, I43T (two isolates), D111A, G112S, and R410W (Table 1). Of these mutations, E40G, I43A, and I43T mapped to the H<sub>2</sub>Pte binding pocket of FolC (Fig. 1). Interestingly, when PAS susceptibility testing was performed for the 8 *folC* mutant strains (Q36, Q93, Q274, Q296, Q449, 1314, 501063, and 504036), those with the E40G, I43A, and I43T mutations (Q36, Q274, Q449, 1314, and 501063) were found to be resistant (Table 1). Thus, H<sub>2</sub>Pte binding pocket mutations are associated with PAS resistance in clinical isolates of *M. tuberculosis*.

**Wild-type *folC* restores PAS susceptibility in PAS<sup>r</sup> *M. tuberculosis* complex strains.** To assess whether the identified *folC* H<sub>2</sub>Pte binding pocket mutations were associated with PAS resistance, a plasmid carrying the wild-type *folC* gene from *M. tuber-*

**TABLE 2** Wild-type *folC* confers PAS susceptibility in laboratory and clinical PAS-resistant *M. tuberculosis* complex strains

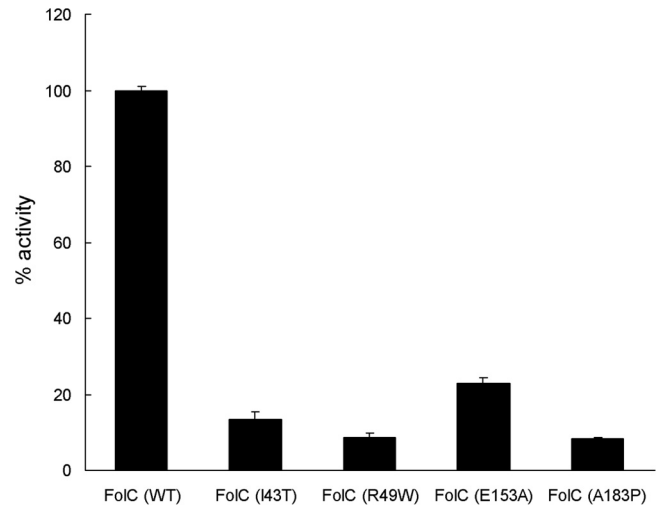
Strain(s)	MICs ( $\mu\text{g/ml}$ ):		
	For PAS	Following transformation with pMV261	Following transformation with pMV261- <i>folC</i>
<i>M. tuberculosis</i> H37Ra	0.125	0.125	0.125
ZF-7, ZF-8, ZF-10, LNE-1 ( <i>folC</i> E153A)	2-4	2-4	0.125
ZF-13, LNE-6 ( <i>folC</i> E153G)	4	4	0.125
ZF-3 ( <i>folC</i> S150G)	8	8	0.125
ZF-4 ( <i>folC</i> F152S)	4	4	0.125
<i>M. bovis</i> BCG	0.125	0.125	0.125
ZF-27, ZF-29 ( <i>folC</i> A183P)	4	4	0.125
ZF-28, ZF-32 ( <i>folC</i> R49W)	4	4	0.125
<i>M. tuberculosis</i> clinical isolates			
Q5 (wild-type <i>folC</i> )	0.5	0.5	0.5
Q36 ( <i>folC</i> I43T)	4	4	1
Q449 ( <i>folC</i> I43A)	>8	>8	1
501063 ( <i>folC</i> E40G)	>8	>8	1

*culosis* H37Rv was used to transform several PAS<sup>r</sup> *M. tuberculosis* H37Ra, *M. bovis* BCG, and *M. tuberculosis* clinical isolates. Plasmid-borne expression of *folC* did not affect PAS susceptibility of the parental strains H37Ra and BCG, nor that of a susceptible clinical isolate (Table 2). In contrast, PAS susceptibility was restored in 15 *folC* mutant PAS<sup>r</sup> strains (*M. tuberculosis* ZF-3, ZF-4, ZF-7, ZF-8, ZF-10, ZF-13, ZF-27, ZF-28, ZF-29, ZF-32, LNE-1, LNE-6, Q36, Q449, and 501063) that were tested (Table 2), indicating that modifications in the H<sub>2</sub>Pte binding pocket were responsible for PAS resistance and that the wild-type enzyme confers PAS susceptibility.

**Replacement of wild-type *folC* with *folC* I43A and I43T confers PAS resistance in *M. tuberculosis* H37Ra.** To further assess the association between PAS resistance and the *folC* H<sub>2</sub>Pte binding pocket mutations I43A and I43T in *M. tuberculosis* clinical isolates Q36 and Q449, *folC* gene replacements were performed with these alleles in *M. tuberculosis* H37Ra. Due to the essentiality of *folC* (24), the gene replacements were achieved by first transforming *M. tuberculosis* H37Ra with an integrative plasmid carrying either the *folC* I43A or I43T allele from PAS<sup>r</sup> clinical isolates and then by subsequently deleting the native copy of *folC* via specialized transduction (17). Deletion of the original copy of the *folC* gene from the genome of *M. tuberculosis* H37Ra was verified by PCR (see Fig. S1 in the supplemental material). The two resultant *M. tuberculosis* H37Ra mutant strains were found to have the same level of PAS resistance (MIC, 8  $\mu\text{g/ml}$ ) as strains Q36 and Q449 (Table 3), demonstrating that the *folC* I43A and I43T alleles were directly

**TABLE 3** *folC* mutations from *M. tuberculosis* clinical isolates confer PAS resistance in *M. tuberculosis* H37Ra

<i>M. tuberculosis</i> strain	MIC ( $\mu\text{g/ml}$ )
H37Ra $\Delta$ <i>folC</i> pMV361- <i>folC</i>	0.125
H37Ra $\Delta$ <i>folC</i> pMV361- <i>folC</i> I43T	8
H37Ra $\Delta$ <i>folC</i> pMV361- <i>folC</i> I43A	8

**FIG 2** DHFS activity of FolC mutants. The DHFS activities of the purified wild-type FolC and FolC mutants were determined using H<sub>2</sub>Pte as the substrate. The enzyme activity was assayed as described in Materials and Methods. The data represent the means  $\pm$  the standard deviations (SD) from three independent experiments.

responsible for PAS resistance in these *M. tuberculosis* clinical isolates.

**FolC H<sub>2</sub>Pte binding pocket variants fail to activate H<sub>2</sub>PtePAS to H<sub>2</sub>PtePAS-Glu.** To better understand the biochemical basis by which FolC H<sub>2</sub>Pte binding pocket variants confer PAS resistance, purified recombinant wild-type FolC and FolC I43T, R49W, E153A, and A183P were assayed for their ability to catalyze the glutamination of H<sub>2</sub>Pte using an HPLC-based method as previously described (7). The retention times of H<sub>2</sub>Pte (substrate) and H<sub>2</sub>Pte-Glu (product) were determined to be 3.88 min and 3.60 min (see Table S2 in the supplemental material). As shown in Fig. 2 and in Fig. S3 in the supplemental material, all FolC variants showed a 5- to 10-fold reduction in DHFS activity relative to the wild-type enzyme, consistent with a defect in native substrate binding.

To assess whether alterations in the H<sub>2</sub>Pte binding pocket also affect the efficiency of H<sub>2</sub>PtePAS glutamination, H<sub>2</sub>PtePAS was synthesized from H<sub>2</sub>PtePP and PAS using purified recombinant FolP1. H<sub>2</sub>PtePAS was purified (see Fig. S4 in the supplemental material) and analyzed by HPLC-MS ([M-H]<sup>-</sup>; peak, *m/z* 329.21) (Fig. 3D). DHFS activity was analyzed using H<sub>2</sub>PtePAS in lieu of H<sub>2</sub>Pte as a substrate. Consistent with previous reports (7, 8), it was found that wild-type FolC catalyzed the ligation of L-glutamate to H<sub>2</sub>PtePAS, yielding H<sub>2</sub>PtePAS-Glu (Fig. 3A and B), which was confirmed by HPLC-MS ([M-H]<sup>-</sup>; peak, *m/z* 458.27) (Fig. 3E). In contrast, all four FolC variants that were tested did not catalyze the formation of detectable H<sub>2</sub>PtePAS-Glu (Fig. 3C). The retention times of H<sub>2</sub>PtePAS and H<sub>2</sub>PtePAS-Glu were determined to be 4.28 min and 4.21 min, respectively (see Table S2 in the supplemental material). In addition, the catalytic rates of wild-type FolC for H<sub>2</sub>Pte and H<sub>2</sub>PtePAS were compared. As shown in Fig. S5 in the supplemental material, under the same conditions, the transformation from H<sub>2</sub>Pte to H<sub>2</sub>PtePAS was completed within 15 min, whereas only about 20% of the H<sub>2</sub>PtePAS was transformed into H<sub>2</sub>PtePAS-Glu after 15 min of incubation.

**H<sub>2</sub>Pte antagonizes the effect of PAS in *M. tuberculosis* H37Ra.** Since PAS acts as an alternative substrate for FolP by com-

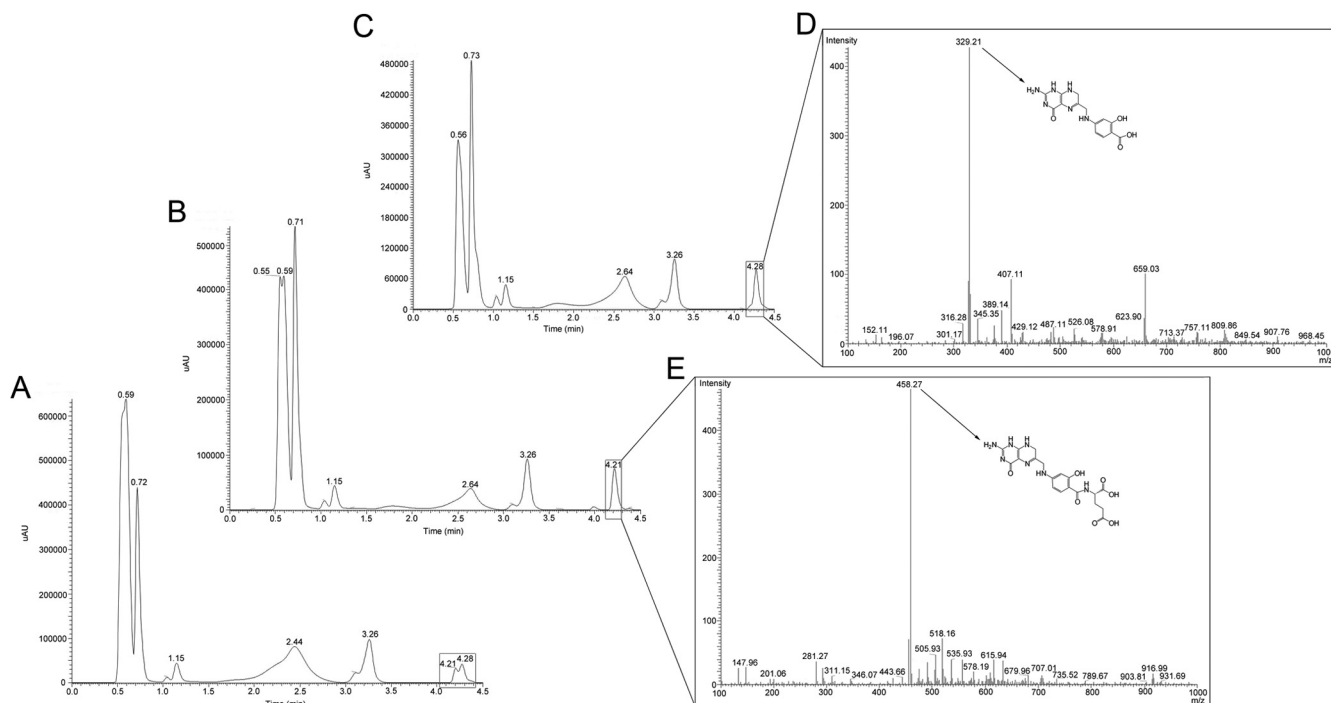


**FIG 3** HPLC-MS analysis of H<sub>2</sub>PtePAS and H<sub>2</sub>PtePAS-Glu. (A) H<sub>2</sub>PtePAS and H<sub>2</sub>PtePAS-Glu coexisted in the reaction system when not all of the H<sub>2</sub>PtePAS was consumed by wild-type FolC. (B and C) Wild-type FolC could catalyze ligation of glutamate to H<sub>2</sub>PtePAS to produce H<sub>2</sub>PtePAS-Glu in the presence of ATP and Mg<sup>2+</sup> (B); however, the FolC mutants could not catalyze this reaction (C). (D) For H<sub>2</sub>PtePAS, the calculated weight was 330.30 and found weight was ~329.21 ([M-H]<sup>-</sup>). (E) For H<sub>2</sub>PtePAS-Glu, the calculated weight was 459.42 and found weight was ~458.27 ([M-H]<sup>-</sup>). All MS data were acquired in the negative mode.

peting with PABA, we wondered whether H<sub>2</sub>Pte could antagonize the effect of PAS. As shown in Fig. 4, the growth inhibitory effects of PAS (0.1 μg/ml) were antagonized by H<sub>2</sub>Pte in a dose-dependent manner, with full antagonism at a concentration of 10 μg/ml H<sub>2</sub>Pte. In addition, the MIC of PAS for *M. tuberculosis* H37Ra was

tested in the presence of H<sub>2</sub>Pte. In the presence of 3 μg/ml H<sub>2</sub>Pte, the MIC of PAS was determined to be to 1 μg/ml, and it increased to 4 μg/ml in the presence of 10 μg/ml H<sub>2</sub>Pte. The interaction between H<sub>2</sub>Pte-Glu and PAS was also tested in *M. tuberculosis* H37Ra; however, H<sub>2</sub>Pte-Glu did not antagonize the effect of PAS.

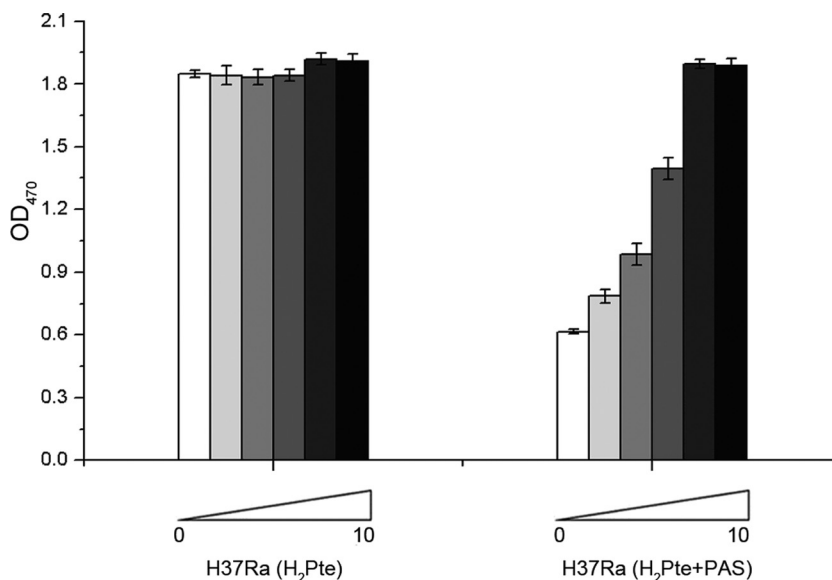


**FIG 4** H<sub>2</sub>Pte antagonized the effect of PAS on *M. tuberculosis* H37Ra. The survival of the bacterial cells after 36 h of treatment was determined by the XTT reduction assay as described in Materials and Methods. H37Ra (H<sub>2</sub>Pte) indicates that bacterial cells were treated with H<sub>2</sub>Pte at different concentrations (0, 0.1, 0.3, 1, 3, and 10 μg/ml), while H37Ra (H<sub>2</sub>Pte + PAS) indicates that bacterial cells were treated with both H<sub>2</sub>Pte (0, 0.1, 0.3, 1, 3, and 10 μg/ml) and PAS (0.1 μg/ml). The data represent the means (bars) ± the SD (error bars) from three independent experiments.

This may be explained in part by the lack of a sufficient transport system for H<sub>2</sub>Pte-Glu in *M. tuberculosis*.

## DISCUSSION

Over the last several years, considerable effort has been made to understand the mechanistic basis for susceptibility and resistance of *M. tuberculosis* to PAS. Evidence for an interaction of this drug with folate metabolism first came from the observation that one-third of PAS-resistant *M. tuberculosis* and *M. bovis* clinical isolates harbored loss-of-function mutations in *thyA* (9). While this result was corroborated by subsequent studies (11, 12), resistance mutations in the remaining two-thirds of PAS-resistant clinical isolates were not defined. Recently, Zheng et al. (8) described a spontaneous PAS-resistant *M. tuberculosis* laboratory isolate in which resistance was conferred by a point mutation in *folC*, indicating that other genes of folate metabolism can contribute to PAS resistance in *M. tuberculosis*.

To identify additional PAS resistance alleles, we genetically characterized several spontaneously resistant mutants of both *M. tuberculosis* H37Ra and *M. bovis* BCG. Using whole-genome and targeted sequencing of 66 PAS-resistant strains, 70% of isolates were found to contain substitution mutations in *folC*. The linkage of these mutations to the PAS-resistant phenotype was confirmed by *folC* complementation and by allelic transfer studies. Sequencing of other genes (including *thyA*, *folP1*, and *dfrA*) in the folate pathway revealed that 10% of the strains had mutations in the *thyA* gene. As 20% of the PAS-resistant strains did not have mutations in genes associated with PAS resistance, additional resistance alleles await identification.

To confirm whether *folC* mutations were associated with PAS resistance in *M. tuberculosis* clinical isolates, 95 *M. tuberculosis* clinical isolates (including 85 MDR isolates) were collected, and the sequences of *folC* in these strains were analyzed. Eight of the MDR strains were found to have five different *folC* mutations, whereas the 10 drug-susceptible strains demonstrated no such mutations. Five of the *folC* mutant strains (Q36, Q274, Q449, 1314, and 501063) were chosen for PAS susceptibility testing and were confirmed to be resistant to PAS. Complementation of *folC* restored PAS susceptibility in all strains that were tested. Further, gene replacement studies in *M. tuberculosis* H37Ra with two mutant *folC* genes derived from two PAS-resistant clinical isolates (Q36 and Q449) showed a direct association of these alleles with clinical PAS resistance. Thus, our data from *M. tuberculosis* H37Ra, *M. bovis* BCG, and MDR *M. tuberculosis* clinical isolates confirm that the *folC* mutation causes PAS resistance in both *M. bovis* and *M. tuberculosis*.

Recently, Chakraborty et al. (7) found that PAS can act as an alternative substrate in *M. tuberculosis* folate metabolism. In this study, it was demonstrated that DHPS (FolP1) can utilize PAS in lieu of PABA in the formation of H<sub>2</sub>PtePAS. Subsequently, H<sub>2</sub>PtePAS can be glutaminated by DHFS (FolC) to yield H<sub>2</sub>PtePAS-Glu (7). These data suggest that PAS may be a prodrug that requires activation through biotransformation by the folate biosynthesis pathway of *M. tuberculosis*. More recently, Zheng et al. (8) demonstrated that H<sub>2</sub>PtePAS-Glu can inhibit the enzymatic activity of dihydrofolate reductase (DHFR), and overexpression of DHFR in *M. tuberculosis* can confer PAS resistance. Together, these observations indicate that PAS is a prodrug that ultimately targets DHFR.

To better understand the mechanistic basis for FolC-linked

PAS resistance, we assessed whether the FolC variants were altered in their enzymatic activities. Consistent with previous reports (7, 8), recombinant wild-type *M. tuberculosis* FolP1 and FolC were able to utilize PAS and H<sub>2</sub>PtePAS, respectively, as a substrate. Yet the rate of DHFS activity with H<sub>2</sub>PtePAS as a substrate for FolC was considerably lower than when H<sub>2</sub>Pte was used as a substrate. When DHFS activities in four recombinant FolC variants (I43T, R49W, E153A, and A183P) were tested with H<sub>2</sub>Pte as a substrate, it was found that all four had reduced activities (from 8% to 22%) relative to the wild-type FolC. Importantly, in contrast to the wild-type enzyme, no H<sub>2</sub>PtePAS-Glu was detected from the FolC variant reaction mixtures, even when the reaction times were extended to 20 h. Consistent with these observations, we found that the addition of H<sub>2</sub>Pte into the growth medium antagonizes the effect of PAS on *M. tuberculosis* H37Ra in a dose-dependent manner. Since H<sub>2</sub>Pte is the natural substrate for FolC and is an analogue of H<sub>2</sub>PtePAS, it can compete with H<sub>2</sub>PtePAS for enzyme binding at high concentrations and block the incorporation of H<sub>2</sub>PtePAS, thus antagonizing the effect of PAS. Together, these data indicate that *folC*-linked PAS resistance is mediated by altered substrate specificity that results in the failure to generate levels of H<sub>2</sub>PtePAS-Glu that are necessary to inhibit DHFR.

To understand why PAS resistance mutations in *folC* led to a decrease in DHFS enzymatic activity, an analysis was performed using previously solved crystal structures of FolC from *M. tuberculosis* and other bacterial species (23). *M. tuberculosis* FolC shows a very similar three-dimensional (3D) structure to those of FolC from *L. casei*, *T. maritima*, *Y. pestis* and *E. coli*. In general, FolC from *M. tuberculosis* has two domains, the amino terminal ATPase domain and the C-terminal Rossmann-fold domain. The N-terminal domain (residues 1 to 334) is composed of one  $\beta$ -sheet with six parallel strands and one anti-parallel strand in the center flanked by nine  $\alpha$ -helices. One central six-stranded  $\beta$ -sheet and five  $\alpha$ -helices constitute the C-terminal domain (residues 342 to 489). Of the structure, the  $\alpha$ 1- $\alpha$ 2 loop (residues 36 to 50) of the FolC N-terminal domain was shown to be involved in H<sub>2</sub>Pte binding (21, 23). Also, the  $\alpha$ 1- $\alpha$ 2 and the  $\alpha$ 4- $\alpha$ 5 loop form a four-helix bundle through hydrophobic interactions. Since the  $\alpha$ 1- $\alpha$ 2 loop is involved in H<sub>2</sub>Pte binding, the four-helix bundle may be functionally important for interaction with H<sub>2</sub>Pte. Among the four residues tested, I43 and R49 reside within the  $\alpha$ 1- $\alpha$ 2 loop, A183 is involved in the linkage of hydrophobic networks between  $\alpha$ 1 and  $\alpha$ 5, and E153 is closely proximal to F152, which is also involved in the linkage of hydrophobic networks between  $\alpha$ 1 and  $\alpha$ 5. Thus, mutations in these four residues may impair H<sub>2</sub>Pte binding, leading to a decrease in enzymatic activity. In fact, all *folC* mutations identified, except N73, are located within the four-helix bundle, so they might also affect H<sub>2</sub>Pte binding and lead to a decrease in enzymatic activity. Previous analysis showed that N73 is involved in nucleoside binding, so a mutation in this residue may affect ATP hydrolysis and consequently reduce the enzymatic activity as well (23).

Taken together, our data demonstrate that the mutation of FolC results in reduced DHFS activity, leading to a blockage of PAS bioactivation and thereby causing PAS resistance in both *M. bovis* and *M. tuberculosis*. A confirmation of this novel mechanism of PAS resistance in mycobacteria, as summarized in Fig. 5, should enable a molecular diagnosis of PAS resistance in clinical isolates and also provide a better understanding of the PAS mode of action in mycobacteria. Our data, in combination with previous reports,

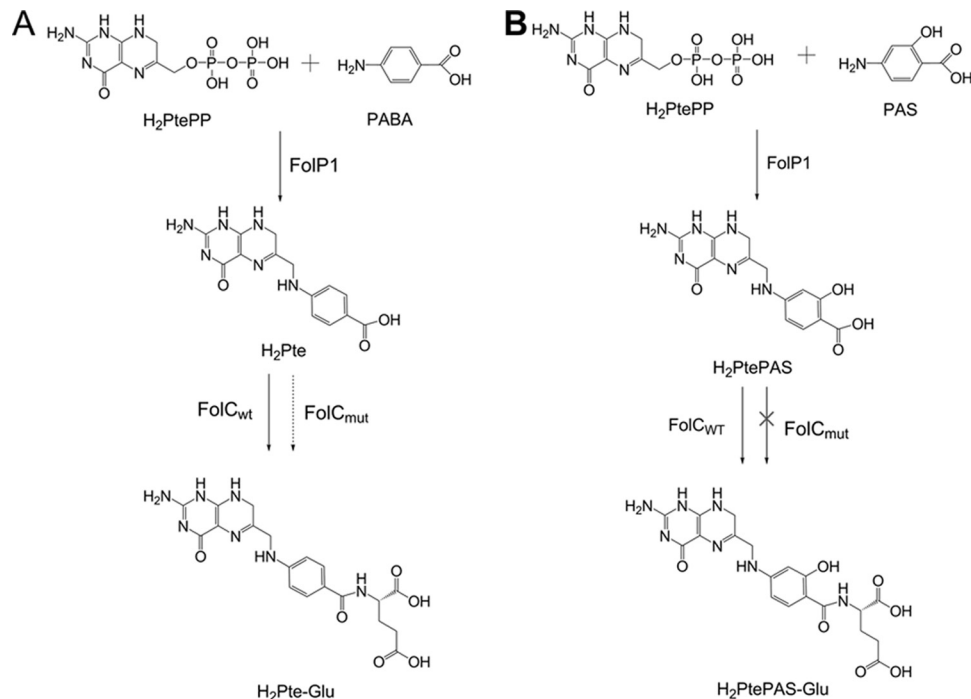


**FIG 5** Schematic of FolC-mediated PAS resistance in *M. bovis* and *M. tuberculosis*. PAS is incorporated into the folate pathway by FolP1 via competition with PABA, yielding H<sub>2</sub>PtePAS. (A) Both wild-type FolC and the FolC mutants can catalyze the formation of H<sub>2</sub>Pte-Glu. (B) In the case of H<sub>2</sub>PtePAS, the wild-type FolC further incorporates it to produce H<sub>2</sub>PtePAS-Glu, whereas the FolC mutants do not. FolC<sub>wt</sub>, wild-type FolC; FolC<sub>mut</sub>, FolC mutants. The dotted arrow indicates the enzymatic activities of the FolC mutants are greatly reduced compared with that of wild-type FolC, and the fork indicates that this pathway is blocked.

clearly demonstrate that PAS action is closely linked with folate metabolism in mycobacteria. Bacteria, fungi, and plants can synthesize folate *de novo* from GTP and chorismate as precursors, while mammals lack this pathway and must obtain folates from their diets (25). Hence, the folate pathway represents an ideal target for designing antimicrobial drugs. For example, FolP1 is the target of important antimicrobial agents, such as sulfonamides and dapson, which are structural analogs of PABA (26). A better understanding of the mode of PAS action and the mechanisms of PAS resistance will be very helpful for the development of new compounds to target *M. tuberculosis* folate metabolism.

#### ACKNOWLEDGMENTS

This work was supported by the State Key Development Program for Basic Research of China (grant no. 2012CB518802 and 2009CB522605), the National Natural Science Foundation of China (grant no. 31300050), and institutional startup funds to A.D.B. from the University of Minnesota.

The Key Laboratory of Agricultural and Environmental Microbiology, Wuhan Institute of Virology, Chinese Academy of Sciences, Wuhan, China, and the State Key Laboratory of Agricultural Microbiology, College of Life Science and Technology, Huazhong Agricultural University, Wuhan, China, contributed equally to this work.

We thank William R. Jacobs, Jr., for providing *M. tuberculosis* H37Ra, *M. bovis* BCG, and *M. smegmatis* mc<sup>2</sup>155, Peng Gong for technical help with structural biology analysis, and Guofeng Zhu for providing the expression plasmids pMV261 and pMV361.

#### REFERENCES

- Dye C, Scheele S, Dolin P, Pathania V, Raviglione MC. 1999. Consensus statement. Global burden of tuberculosis: estimated incidence, prevalence, and mortality by country. *JAMA* 282:677–686. <http://dx.doi.org/10.1001/jama.282.7.677>.
- Gandhi NR, Moll A, Sturm AW, Pawinski R, Govender T, Lalloo U, Zeller K, Andrews J, Friedland G. 2006. Extensively drug-resistant tuberculosis as a cause of death in patients co-infected with tuberculosis and HIV in a rural area of South Africa. *Lancet* 368:1575–1580. [http://dx.doi.org/10.1016/S0140-6736\(06\)69573-1](http://dx.doi.org/10.1016/S0140-6736(06)69573-1).
- World Health Organization. 2012. Global tuberculosis report 2012. World Health Organization, Geneva, Switzerland. [http://apps.who.int/iris/bitstream/10665/75938/1/9789241564502\\_eng.pdf](http://apps.who.int/iris/bitstream/10665/75938/1/9789241564502_eng.pdf).
- Lehmann J. 1946. *para*-Aminosalicylic acid in the treatment of tuberculosis. *Lancet* 247:15. [http://dx.doi.org/10.1016/S0140-6736\(46\)91185-3](http://dx.doi.org/10.1016/S0140-6736(46)91185-3).
- Youmans GP, Raleigh GW, Youmans AS. 1947. The tuberculostatic action of *para*-aminosalicylic acid. *J. Bacteriol.* 54:409–416.
- Nopponpunch V, Sirawaraporn W, Greene PJ, Santi DV. 1999. Cloning and expression of *Mycobacterium tuberculosis* and *Mycobacterium leprae* dihydropteroate synthase in *Escherichia coli*. *J. Bacteriol.* 181:6814–6821.
- Chakraborty S, Gruber T, Barry CE, III, Boshoff HI, Rhee KY. 2013. *para*-Aminosalicylic acid acts as an alternative substrate of folate metabolism in *Mycobacterium tuberculosis*. *Science* 339:88–91. <http://dx.doi.org/10.1126/science.1228980>.
- Zheng J, Rubin EJ, Bifani P, Mathys V, Lim V, Au M, Jang J, Nam J, Dick T, Walker JR, Pethe K, Camacho LR. 2013. *para*-Aminosalicylic acid is a prodrug targeting dihydrofolate reductase in *Mycobacterium tuberculosis*. *J. Biol. Chem.* 288:23457–23456. <http://dx.doi.org/10.1074/jbc.P113.475798>.
- Rengarajan J, Sasseti CM, Naroditskaya V, Sloutsky A, Bloom BR, Rubin EJ. 2004. The folate pathway is a target for resistance to the drug *para*-aminosalicylic acid (PAS) in mycobacteria. *Mol. Microbiol.* 53:275–282. <http://dx.doi.org/10.1111/j.1365-2958.2004.04120.x>.
- Fivian-Hughes AS, Houghton J, Davis EO. 2012. *Mycobacterium tuberculosis* thymidylate synthase gene *thyX* is essential and potentially bifunctional, while *thyA* deletion confers resistance to *p*-aminosalicylic acid. *Microbiology* 158:308–318. <http://dx.doi.org/10.1099/mic.0.053983-0>.
- Mathys V, Wintjens R, Lefevre P, Bertout J, Singhal A, Kiass M, Kurepina N, Wang XM, Mathema B, Baulard A, Kreiswirth BN, Bifani

- P. 2009. Molecular genetics of *para*-aminosalicylic acid resistance in clinical isolates and spontaneous mutants of *Mycobacterium tuberculosis*. *Antimicrob. Agents Chemother.* 53:2100–2109. <http://dx.doi.org/10.1128/AAC.01197-08>.
12. Zhang Z, Zhao Y, Li Z, Jia H, Liu Y, Chen X, Liu Z, Du B, Xing A, Ma Y. 2007. Mutations in the thymidylate synthase gene is a major mechanism in the *para*-aminosalicylic acid resistance of *M. tuberculosis*. *Zhonghua Jie He He Hu Xi Za Zhi.* 30:683–685. (In Chinese.)
  13. Kim SJ, Hong YP. 1992. Drug resistance of *Mycobacterium tuberculosis* in Korea. *Tuber. Lung Dis.* 73:219–224. [http://dx.doi.org/10.1016/0962-8479\(92\)90090-7](http://dx.doi.org/10.1016/0962-8479(92)90090-7).
  14. Larsen MH, Biermann K, Tandberg S, Hsu T, Jacobs WR, Jr. 2007. Genetic manipulation of *Mycobacterium tuberculosis*. *Curr. Protoc. Microbiol.* Chapter 10:Unit 10A.2. <http://dx.doi.org/10.1002/9780471729259.mc10a02s6>.
  15. Wang XD, Gu J, Wang T, Bi LJ, Zhang ZP, Cui ZQ, Wei HP, Deng JY, Zhang XE. 2011. Comparative analysis of mycobacterial NADH pyrophosphatase isoforms reveals a novel mechanism for isoniazid and ethionamide inactivation. *Mol. Microbiol.* 82:1375–1391. <http://dx.doi.org/10.1111/j.1365-2958.2011.07892.x>.
  16. Li R, Yu C, Li Y, Lam TW, Yiu SM, Kristiansen K, Wang J. 2009. SOAP2: an improved ultrafast tool for short read alignment. *Bioinformatics* 25:1966–1967. <http://dx.doi.org/10.1093/bioinformatics/btp336>.
  17. Bardarov S, Bardarov S, Jr, Pavelka MS, Jr, Sambandamurthy V, Larsen M, Tufariello J, Chan J, Hatfull G, Jacobs WR, Jr. 2002. Specialized transduction: an efficient method for generating marked and unmarked targeted gene disruptions in *Mycobacterium tuberculosis*, *M. bovis* BCG and *M. smegmatis*. *Microbiology* 148:3007–3017.
  18. Singh U, Akhtar S, Mishra A, Sarkar D. 2011. A novel screening method based on menadione mediated rapid reduction of tetrazolium salt for testing of anti-mycobacterial agents. *J. Microbiol. Methods* 84:202–207. <http://dx.doi.org/10.1016/j.mimet.2010.11.013>.
  19. Sun X, Bogнар AL, Baker EN, Smith CA. 1998. Structural homologies with ATP- and folate-binding enzymes in the crystal structure of folylpolyglutamate synthetase. *Proc. Natl. Acad. U. S. A.* 95:6647–6652. <http://dx.doi.org/10.1073/pnas.95.12.6647>.
  20. Sheng Y, Cross JA, Shen Y, Smith CA, Bogнар AL. 2002. Mutation of an essential glutamate residue in folylpolyglutamate synthetase and activation of the enzyme by pteroyl binding. *Arch. Biochem. Biophys.* 402:94–103. [http://dx.doi.org/10.1016/S0003-9861\(02\)00040-1](http://dx.doi.org/10.1016/S0003-9861(02)00040-1).
  21. Mathieu M, Debousker G, Vincent S, Viviani F, Bamas-Jacques N, Mikol V. 2005. *Escherichia coli* FolC structure reveals an unexpected dihydrofolate binding site providing an attractive target for anti-microbial therapy. *J. Biol. Chem.* 280:18916–18922. <http://dx.doi.org/10.1074/jbc.M413799200>.
  22. Smith CA, Cross JA, Bogнар AL, Sun X. 2006. Mutation of Gly51 to serine in the P-loop of *Lactobacillus casei* folylpolyglutamate synthetase abolishes activity by altering the conformation of two adjacent loops. *Acta Crystallogr. D Biol. Crystallogr.* 62:548–558. <http://dx.doi.org/10.1107/S0907444906009796>.
  23. Young PG, Smith CA, Metcalf P, Baker EN. 2008. Structures of *Mycobacterium tuberculosis* folylpolyglutamate synthase complexed with ADP and AMPPCP. *Acta Crystallogr. D Biol. Crystallogr. D.* 64:745–753. <http://dx.doi.org/10.1107/S0907444908012262>.
  24. Sasseti CM, Boyd DH, Rubin EJ. 2003. Genes required for mycobacterial growth defined by high density mutagenesis. *Mol. Microbiol.* 48:77–84. <http://dx.doi.org/10.1046/j.1365-2958.2003.03425.x>.
  25. Gregory JF, III. 1989. Chemical and nutritional aspects of folate research: analytical procedures, methods of folate synthesis, stability, and bioavailability of dietary folates. *Adv. Food Nutr. Res.* 33:1–101.
  26. Anand N. 1975. Sulfonamides and sulfones, p 668–698. *In* Corcoran JW, Hahn FE, Snell JF, Arora KL (ed), *Mechanism of action of antimicrobial and antitumor agents*. Springer-Verlag, New York, NY.